Res Chem Intermed (2013) 39:1655–1664
DOI 10.1007/s11164-012-0899-9

One-step synthesis of nanocrystalline N-doped TiO_2 powders and their photocatalytic activity under visible light irradiation

Junna Xu · Qing Liu · Shufeng Lin · Wenbin Cao

Received: 31 March 2012 / Accepted: 22 July 2012 / Published online: 10 November 2012

Abstract Nanocrystalline N-doped TiO_2 powders were successfully prepared by hydrothermal reaction for 2 h at low temperature (120 °C) and at an applied pressure of 3 MPa. The grain size of the powders (calculated by use of Scherrer's method) ranged from 8.2 to 10.2 nm. The BET specific surface area ranged from 151.0 to 220.0 m^2/g. A significant shift of the light absorption edge toward the visible light zone was observed in the UV–visible spectra. XPS results showed that nitrogen atoms were incorporated into the TiO_2 lattice. The photocatalytic activity of the synthesized N-doped TiO_2 powders was evaluated by measurement of photodegradation of methylene blue (MB) in aqueous solution under visible light irradiation. The amount of MB degraded increased with increasing illumination intensity.

Keywords N-TiO_2 · Hydrothermal method · Photocatalysis

J. Xu · Q. Liu · S. Lin · W. Cao (✉)
Department of Inorganic Nonmetallic Materials, School of Materials Science and Engineering, University of Science and Technology Beijing, Beijing 100083, China
e-mail: wbcao@ustb.edu.cn

J. Xu
e-mail: xujunna83@163.com

Q. Liu
e-mail: cathie811@126.com

S. Lin
e-mail: linshufeng1987@yahoo.com.cn

J. Xu · Q. Liu · S. Lin · W. Cao
State Key Laboratory of High Performance Ceramics and Superfine Microstructure, Shanghai Institute of Ceramics, Chinese Academy of Sciences, Shanghai, China

Introduction

Titanium dioxide is one of the most promising photocatalysts because of its low cost, non-toxicity, photostability, and high photocatalytic efficiency. However, titanium dioxide can be excited only by ultraviolet light because of its wide bandgap (3.2 eV for anatase). Substitution doping with transition metals (Cr [1], Fe [2], Mo [3], W [4], V [5] etc.) and nonmetals (N [6], C [7], S [8], P [9] etc.) is regarded as a very promising way of extending its optical response to visible light and improving its photocatalytic performance. Nitrogen doping has attracted much attention because of its atomic size comparable with that of oxygen, metastable center formation, and small ionization energy [10]. Different strategies have been used to prepare N-doped TiO_2. However, those methods usually involve high temperature [11, 12] or a complex synthetic process [13]. In the work discussed in this paper, nanocrystalline N-doped TiO_2 powders were prepared by a mild hydrothermal method at low temperature in a simple process without post-calcination for crystallization. The phase composition, morphology, surface area, valence state, and light absorption of the synthesized samples were characterized by XRD, TEM, BET, XPS, and UV–visible diffusion reflectance spectroscopy. The photocatalytic performance of the N-doped TiO_2 nanoparticles was evaluated by measurement of photodegradation of methylene blue (MB) in aqueous solution.

Experimental

Synthesis of N-doped TiO_2 powders by hydrothermal method

Technical grade titanyl sulfate, urea, and guanidine hydrochloride were used as starting materials. All were commercially available materials and were used as received. In a typical synthesis, the desired amounts of titanyl sulfate, urea, and guanidine hydrochloride were mixed with 1 L distilled water and the suspension was placed in a Teflon-lined autoclave of internal volume of 2 L. The chamber was flushed with nitrogen gas at a pressure of 3 MPa and stirred at 300 r/min. The autoclave was heated to 120, 130, or 150 °C for 2 h (designated TN120, TN130, and TN150, respectively). The synthesized products were cooled to room temperature, centrifuged, and washed with distilled water several times until SO_4^{2-} and other ions were not detected in the washings. The solids were dried at 90 °C in air to give the desired powders. Non-doped TiO_2 was prepared by the same procedure at 150 °C (designated T150).

Characterization

The phase composition of the as-synthesized N-doped TiO_2 powders was determined by X-ray diffraction with a Cu Kα source in the 2θ range 20–80°. Grain size was estimated by use of Scherrer's method. The Brunauer–Emment–

Teller (BET) surface area of the powders was measured by nitrogen adsorption at 77 K, by use of a Quantasorb-18 apparatus. The morphology of the samples was characterized by transmission electron microscopy (TEM, Hitachi, Jeol 200CX). The UV–visible diffuse reflectance spectra of the powders, in the range 250–700 nm, were recorded on a Pgeneral UV-1901 instrument. The surface composition and valence state of the powders were determined by X-ray photoelectron spectroscopy (XPS, Escalab 250). Fourier transform infrared spectra in the range 4,000–400 cm^{-1} were acquired with a Thermo Nicolet Nexus 670 spectrometer.

Photodegradation of MB in aqueous solution

Typically, 1 g synthesized N-doped TiO_2 powder was used to degrade 100 mL MB aqueous solution, concentration 10 mg/L, under visible light irradiation. After addition of the powder to the solution, the suspension was homogenized by stirring continuously in dark for 2 h. Two lamps, each of power 23 watt (illuminance 15,000 Lux) were used for irradiation. The concentration of MB at the start of photodegradation ($t = 0$) was designated C_0. The suspension was sampled at 2 h intervals and centrifuged to remove the TiO_2 particles. The concentration of MB (C) in each sample was determined by measuring the absorbance of the solutions, by UV–visible spectrophotometry, at $\lambda_{max} = 664$ nm.

Results and discussion

Pure synthesized TiO_2 powder was white whereas the color of N-doped TiO_2 powders changed from dark yellow to light yellow with increasing reaction temperature. Figure 1 shows the XRD patterns of samples synthesized at different reaction temperatures. All the peaks of the XRD patterns correspond to those of anatase. No peaks of TiN or other compounds are detected. The intensities of the peaks become greater with increasing reaction temperature, because of improvement of the crystallinity. The grain sizes calculated by use of Scherer's formula are 10.2, 8.2, 8.5, and 10 nm for samples T150, TN120, TN130, and TN150, respectively. The TEM micrograph of TN150, shown in Fig. 2, indicates the particles were approximately spherical in shape and approximately 11 nm in size, which is consistence with the results from Scherrer's method.

Figure 3 shows the BET surface areas of samples prepared at different reaction temperatures. The surface area tends to decrease with increasing reaction temperature because of the increasing grain size and better crystallinity. TN120 has the largest surface area of 220 m^2/g. The surface areas of samples TN130 and TN150 were 198 and 155 m^2/g, respectively, whereas that of sample T150 is 151 m^2/g.

Figure 4a shows the UV–visible diffusion reflectance spectra of the samples. It is clear that N-doped TiO_2 absorbs visible light more strongly. The reflectance data are converted to the absorption coefficient values $F(R_\infty)$by use of the Kubelka–Munk equation:

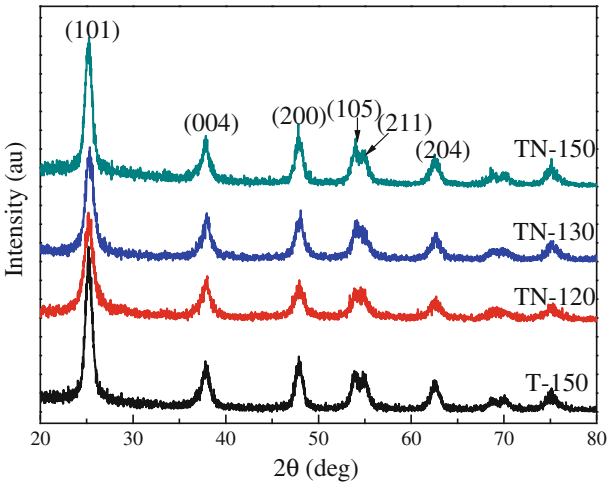

Fig. 1 XRD patterns obtained from samples synthesized at different reaction temperatures

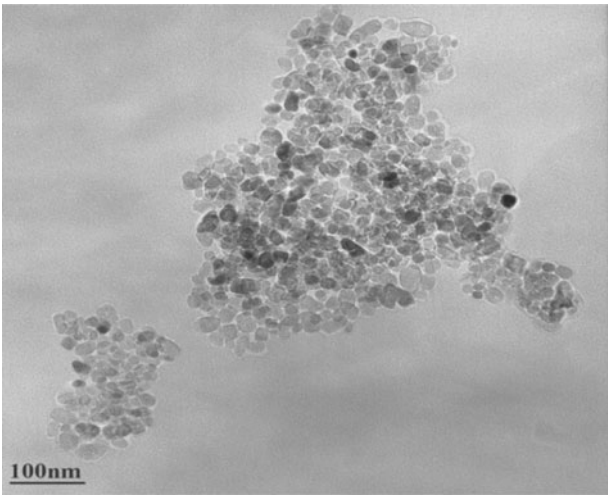

Fig. 2 TEM micrograph of TN150

$$F(R_\infty) = \frac{(1 - R_\infty)^2}{2R_\infty} \tag{1}$$

N-doped TiO_2 and TiO_2 have been treated as indirect semi-conductors [14]. A modified Kubelka–Munk function can be constructed by plotting $(F(R_\infty)hv)^{0.5}$ against the energy excitation $E(hv)$ to calculate the band gap, as shown in Fig. 4b. Estimated band gap energies are 3.2, 3.02, 3.08, and 2.97 eV for T150, TN150, TN130, and TN120, respectively.

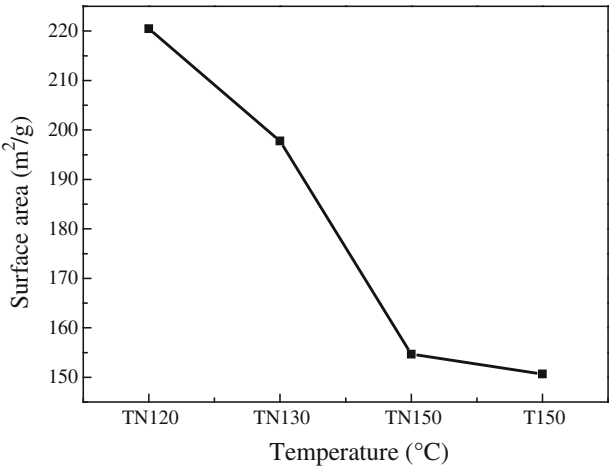

Fig. 3 BET surface area of samples synthesized at different reaction temperatures

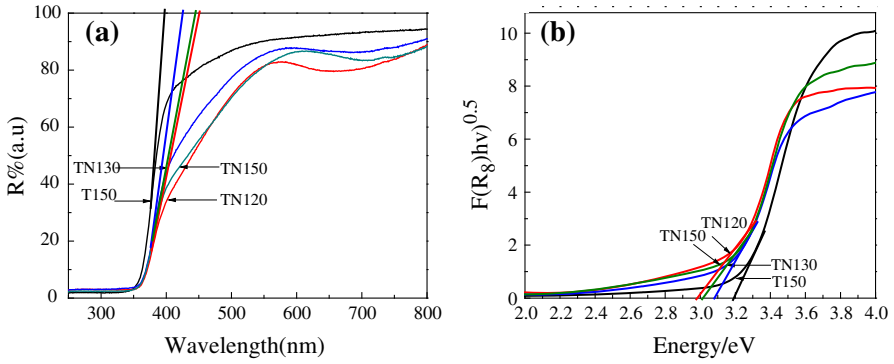

Fig. 4 UV–visible diffusion reflectance spectra (**a**) and modified Kubelka–Munk function vs excited energy (**b**) of the samples

The element composition and the valence state of TN150 were investigated by XPS, as shown in Fig. 5. The survey spectrum shows the surface of TN150 is composed of Ti, O, N, and C. The concentration of nitrogen is approximately 0.8 at.%. Asahi [15] believed the narrower band gap could be attributed to mixing of the N2p and O2p states whereas Irie [16] indicated that isolated N2p states located above the O2p valance band might lead to the visible light sensitivity. Yang [17] suggested that when the concentration of dopant was below 2.1 at.%, the substitutional N atoms would introduce N2p states above the valence band, which might contribute to narrowing the band gap energy. Figure 5b shows the binding energy of N1s at 396.2 and 399.8 eV. The N1s peak located between 396 and 397 eV is usually attributed to the substitution of oxygen by nitrogen in the TiO_2 lattice and formation of Ti–N bonds [18–20]. Thus the occurrence of the N1s peak at 396.2 eV indicates that nitrogen atoms have been incorporated into the TiO_2

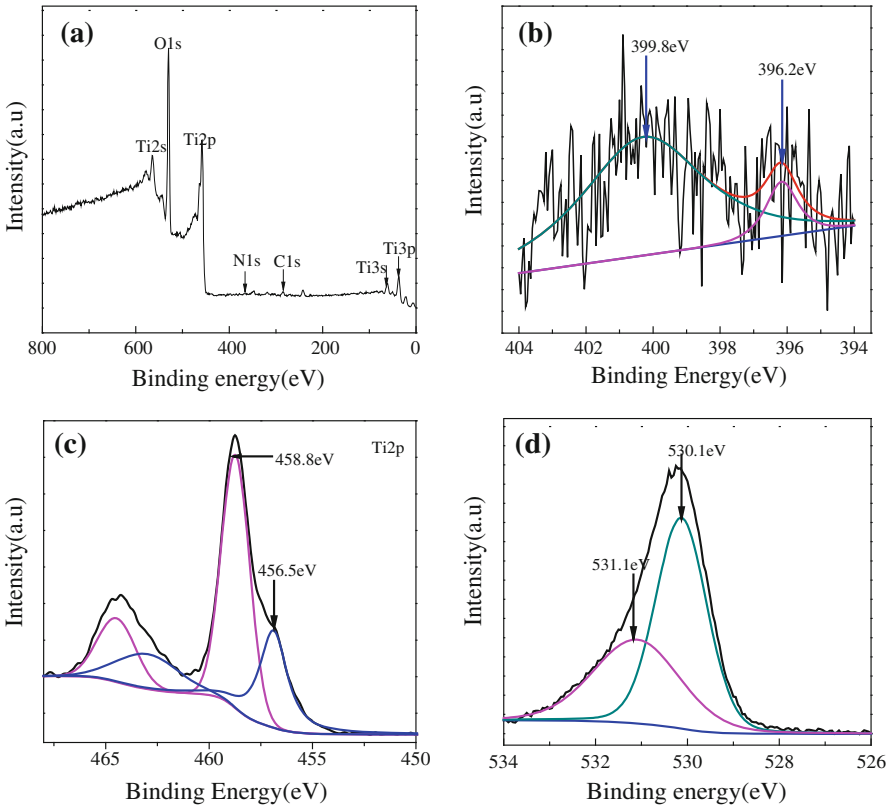

Fig. 5 XPS spectra of TN150: (**a**) survey spectrum, (**b**) N1s, (**c**) Ti2p, (**d**) O1s

lattice. Huang [21] proposed that nitrogen atoms substituted oxygen atoms in the nucleation process during the hydrothermal procedure. The nature of the N1s peak at approximately 400 eV is still controversial. Asahi [15] attributed this peak to chemisorption of N_2 molecules whereas Yang [22] attributed N1s peaks at 399.45 and 401.5 eV to O–Ti–N and Ti–O–N bonds, respectively. Xiang [23, 24] ascribed the N1s peak at 400 eV to interstitial nitrogen atoms in the TiO_2 lattice and to formation of Ti–N–O bonds.

The method of preparation and the source of nitrogen may also affect doping of the TiO_2 lattice with nitrogen [25–27]. Generally, magnetron sputtering [15, 28], calcination [16, 29, 30], and ion implantation [31, 32] are regarded as effective means of preparation of substitutional nitrogen-doped TiO_2 whereas sol–gel [27], microwave [25], and hydrothermal [26, 26] methods are regarded as furnishing TiO_2 with interstitial nitrogen (N–TiO_2). However, Jagadale [33] prepared substitutional N-doped TiO_2 by a sol–gel method, and Peng [34] and D'Arienzo [35] achieved substitutional doping of the TiO_2 lattice with nitrogen by use of a hydrothermal method.

We assign the peak at 399.8 eV to a Ti–O–N linkage in TiO_2, which is regarded as interstitial nitrogen. As mentioned above, however, it is still difficult to

characterize how the TiO_2 lattice has been doped with nitrogen, and further theoretical and experimental work is needed for confirmation of this.

The Ti2p peak becomes broader and unsymmetrical after N doping, as indicated in Fig. 5c, the peak at 458.8 eV is attributed to O–Ti–O in TiO_2 [36]. The peak located at 456.5 eV may be attributed to formation of Ti_2O_3 and may be coupled with an oxygen vacancy [5]. The O1s peak at 530.1 eV is ascribed to the Ti–O bond in TiO_2, as shown in Fig. 5d. Nonetheless, an additional peak appears at 531.1 eV. Ou [37] attributed this peak to Ti–OH groups, and Cong [38, 39] assigned it to the presence of Ti–O–N bonds. We ascribe the peak at 531.1 eV to formation of oxidized Ti–N, which is in accordance with the N1s results.

The FTIR spectra of pure TiO_2 and TN150 are shown in Fig. 6. The peaks located at 3,400 and 1,630 cm^{-1} are attributed to stretching and bending vibration of hydroxyl groups [22, 40]. The peak at 1,390 cm^{-1} is assigned to the bending vibration of NH_4^+ [41]. An additional peak at 1,050 cm^{-1} is found in N-doped TiO_2; this could be attributed to nitrogen atoms embedded in the TiO_2 network [42].

Figure 7 shows the effect of irradiation time on the extent of degradation of MB by the synthesized powders. Because MB absorbs visible light [43], its photodegradation under visible light irradiation in the absence of any powder was investigated to exclude any effect of visible light absorption. It can be seen that the MB was hardly decomposed with increasing visible light irradiation time. The concentration of MB also remained almost unchanged when kept in the dark in the presence of TiO_2 powders, which indicates that the effect on photocatalytic activity of adsorption of MB on the powders' surfaces can be ignored. N-doped TiO_2 was more photoactive than pure TiO_2, indicating that nitrogen doping enhances the photocatalytic activity of TiO_2 in the visible light region. Among all the N-doped samples, degradation of MB by TN120 was largest (92 %), indicating TN120 has the best photocatalytic activity. Yang [22] also reported that the photocatalytic

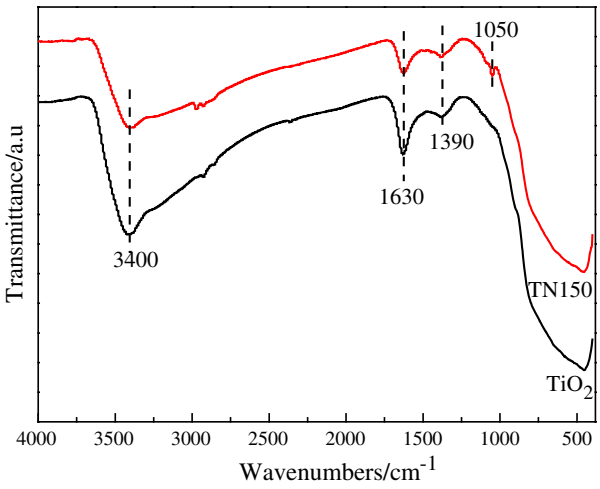

Fig. 6 FTIR spectra of pure TiO_2 and TN150

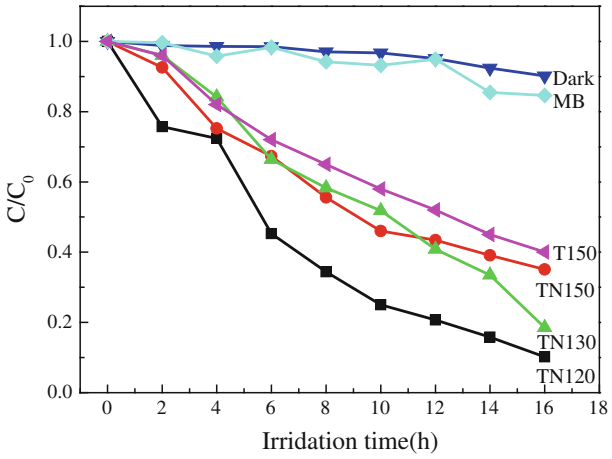

Fig. 7 Effect of irradiation time on the extent of degradation of MB by the synthesized powders

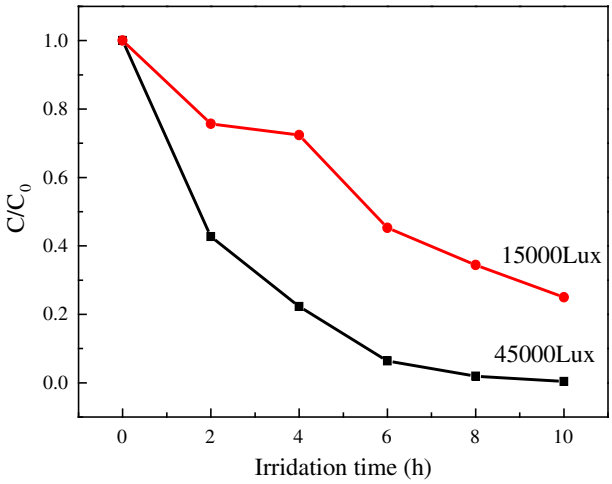

Fig. 8 Photocatalytic degradation of MB by TN120 under different illumination intensity conditions

activity of N-doped TiO_2 decreased with increasing hydrothermal temperature. The larger surface area and the ability to absorb visible light should account for this. Larger surface area favors absorption of hydroxyl groups, which are generated in the photocatalytic reaction and enhance the photocatalytic activity [44]. The doped nitrogen and the resulting oxygen vacancies will behave as holes and electron traps, respectively. Therefore, the rate of recombination of electron–hole pairs could be suppressed [27].

The effect of the intensity of visible light illumination on the extent of photodegradation was also investigated. The results, given in Fig. 8, revealed that the extent of degradation increased from 75 to 100 % when the illumination

intensity was increased from 15,000 to 45,000 Lux, because of the greater number of electron–hole pairs generated on the surface of the photocatalyst.

Conclusion

Nitrogen-doped TiO_2 powders with large BET surface area were successfully prepared by one-step hydrothermal reaction at low temperature. The grain size of the synthesized samples ranged from 8.2 to 10.2 nm and the specific surface area ranged from 151 to 220 m^2/g. Nitrogen atoms were incorporated into the TiO_2 lattice. In the degradation of MB, the sample prepared at 120 °C had much greater photocatalytic activity in visible light than the powders synthesized at other reaction temperatures, because of its higher surface area and narrower band gap.

Acknowledgments This work was financially supported by the National Natural Science Foundation of China (grant no. 51072019), the National High Technology Research and Development Program of China (grant no. 2012AA030302), and the Opening Project of State Key Laboratory of High Performance Ceramics and Superfine Microstructure under the grant SKL201112SIC.

References

1. X.G. Qu, W.X. Liu, J. Ma, D.N. Yu, W.B. Cao, J.H. Mao, Mater. Sci. Forum **620–622**, 703 (2009)
2. J. Ma, Y. Wei, W.X. Liu, W.B. Cao, Res. Chem. Intermed. **35**, 329 (2009)
3. X.H. Yu, C.S. Li, Y. Ling, T.A. Tang, Q. Wu, J.J. Kong, J. Alloys Compd. **50**(7), 33 (2010)
4. Y.T. Song, W.N. Shao, W.B. Cao, 489. Mater. Sci. Forum **695**, 489 (2011)
5. B.S. Liu, X.L. Wang, G.F. Cai, L.P. Wen, Y.B. Song, X.J. Zhao, J. Hazards Mater. **169**, 1112 (2009)
6. Y.H. Li, W.B. Cao, F.Y. Ran, X.N. Zhang, Key Eng. Mater. **336–338**, 1972 (2007)
7. H.Y. Li, D.J. Wang, H.M. Fan, P. Wang, T.F. Jiang, T.F. Xie, J. Colloid Interface Sci. **35**(4), 175 (2011)
8. M. Hamadanian, A. Reisi-Vanani, A. Majedi, Mater. Chem. Phys. **116**, 376 (2009)
9. Y.Y. Lv, L.S. Yu, H.Y. Huang, H.H. Liu, Y.Y. Feng, J. Alloys Compd. **488**, 314 (2009)
10. X.F. Qiu, C. Burda, Chem. Phys. **339**, 1 (2007)
11. B. Baruwati, S. Varma, J. Nanosci. Nanotechnol. **1**(1), 2036 (2011)
12. M. Matsushita, A.Y. Nosaka, J. Nishino, Y. Nosaka, J. Ceram. Soc. Jpn. **11**(2), S1411 (2004)
13. D.Y. Wu, M.C. Long, W.M. Cai, C. Chen, Y.H. Wu, J. Alloys Compd. **502**, 289 (2010)
14. H. Lin, C.P. Huang, W. Li, C. Ni, S. Ismat Shah, Y.-H. Tseng, Appl. Catal. B **6**(8), 1 (2006)
15. R. Asahi, T. Morikawa, T. Ohwaki, K. Aoki, Y. Taga, Science **293**, 269 (2001)
16. H. Irie, Y. Watanabe, K. Hashimoto, J. Phys. Chem. B **107**, 5483 (2003)
17. K. Yang, Y. Dai, B.B. Huang, J. Phys. Chem. C **111**, 12086 (2007)
18. H.Q. Sun, Y. Bai, H.J. Liu, W.Q. Jin, N.P. Xu, G.J. Chen, B.Q. Xu, J. Phys. Chem. C **112**, 13304 (2008)
19. T. Yu, X. Tan, L. Zhao, Y.X. Yin, P. Chen, J. Wei, Chem. Eng. J. **157**, 86 (2010)
20. F. Peng, L.F. Cai, H. Yu, H.J. Wang, J. Yang, J. Solid States Chem. **181**, 130 (2008)
21. D.G. Huang, S.J. Liao, S.Q. Quan, L. Liu, Z.J. He, J.B. Wan, W.B. Zhou, J. Non-Cryst. Solids **354**, 3965 (2008)
22. Q.L. Yang, Y. Sun, J.X. Su, L. Guo, L. Jiang, Mater. renew. energy environ. **2**, 1433 (2011)
23. Q.J. Xiang, J.G. Yu, M. Jaroniec, Phys. Chem. Chem. Phys. **13**, 4853 (2011)
24. Q.J. Xiang, J.G. Yu, W.G. Wang, M. Jaronie, Chem. Commun. **47**, 6906 (2011)
25. H. Diker, C. Varlikli, K. Mizrek, A. Dana, Energy **36**, 1243 (2011)
26. J. Yu, W.G. Wang, B. Cheng, B.L. Su, J. Phys. Chem. C **11**(3), 6743 (2009)
27. J. Ananpattarachai, P. Kajitvichyanukul, S. Seraphin, J. Hazard. Mater. **168**, 253 (2009)
28. J.M. Mwabora, T. Lindgren, E. Avendaño, T.F. Jaramillo, J. Lu, S.E. Lindquist, C.G. Granqvist, J. Phys. Chem. B **108**, 20193 (2004)

29. S. Livraghi, K. Elghniji, A.M. Czoskaa, M.C. Paganini, E. Giamelloa, M. Ksibi, J. Photochem. Photobiol. A **20**(5), 93 (2009)
30. W.B. Cao, Y. Wei, Y.H. Li, X.N. Zhang, Mater. Sci. Forum **544–545**, 167 (2007)
31. O. Diwald, T.L. Thompson, T. Zubkov, E.G. Goralski, S.D. Walck, J.T. Yates Jr., J. Phys. Chem. B **108**, 6004 (2004)
32. O. Diwald, T.L. Thompson, E.G. Goralski, S.D. Walck, J.T. Yates Jr., J. Phys. Chem. B **108**, 52 (2004)
33. T.C. Jagadale, S.P. Takale, R.S. Sonawane, H.M. Joshi, S.I. Patil, B.B. Kale, S.B. Ogale, J. Phys. Chem. C **112**, 14595 (2008)
34. F. Peng, L.F. Cai, L. Huang, H. Yu, H.J. Wang, J. Phys. Chem. Solids **69**, 1657 (2008)
35. M. D'Arienzo, R. Scotti, L. Wahba, C. Battocchio, E. Bemporad, A. Nale, F. Morazzoni, Appl. Catal. B **93**, 149 (2009)
36. M.E. Kurtoglu, T. Longenbach, K. Sohlberg, Y. Gogotsi, J. Phys. Chem. C **115**, 1739 (2011)
37. H.H. Ou, S.L. Lo, C.H. Liao, J. Phys. Chem. C **115**, 4000 (2011)
38. Y. Cong, J.L. Zhang, F. Chen, M. Anpo, J. Phys. Chem. C **11**(1), 6976 (2007)
39. H.Q. Sun, Y. Bai, W.Q. Jin, N.P. Xu, Sol. Energy Mater. Sol. Cells **9**(2), 76 (2008)
40. J. Fang, F.C. Shi, J. Bu, J.J. Ding, S.T. Xu, J. Bao, Y.S. Ma, Z.Q. Jiang, W.P. Zhang, C. Gao, W.X. Huang, J. Phys. Chem. C **11**(4), 7940 (2010)
41. K.M.S. Khalil, M.I. Zaki, Powder Technol. **9**(2), 233 (1997)
42. S.Z. Hu, A.J. Wang, X. Li, J. Phys. Chem. Solids **7**(1), 156 (2010)
43. X.L. Yan, T. Ohno, K. Nishijiama, R. Abe, B. Ohtanl, Chem. Phys. Lett. **429**, 606 (2006)
44. S.Z. Hu, A.J. Wang, X. Li, H. Lowe, J. Phys. Chem. Solids **71**, 156 (2010)